Poly-phosphocholinated Liposomes Form Stable Superlubrication Vectors

(article begins on next page)

Poly-phosphocholinated Liposomes Form Stable Superlubrication Vectors

Weifeng Lin[1], Nir Kampf[1], Ronit Goldberg[1], Michael J. Driver[2], Jacob Klein[1]*

[1]Department of Materials and Interfaces, Weizmann Institute of Science, Rehovot 76100, Israel.
[2] Vertellus Biomaterials, Vertellus Specialties UK Ltd., Basingstoke, Hampshire RG25 2PH, U.K.

*** Corresponding author:**
E-mail address: jacob.klein@weizmann.ac.il

■ **ABSTRACT:** We have prepared phosphatidylcholine (PC) vesicles (liposomes) incorporating a novel lipid/poly-phosphocholine conjugate. This both stabilizes the liposomes against aggregation (for example during storage or when being delivered) and at the same time allows them to act as very efficient lubricating elements readily attaining superlubric performance (defined as coefficient of friction $\mu < 10^{-2}$) via hydration lubrication, at physiological salt concentrations and pressures. In contrast, vesicles sterically-protected by poly(ethylene glycol) chains (PEGylation), which is the general method-of-choice, while equally stable to aggregation, are much poorer lubricants under these conditions, attributed to relatively poor hydration of the PEG. Our approach enables the use of PC liposomes as stable superlubrication vectors in potential biomedical applications.

■ INTRODUCTION

Hydration lubrication, where sub-nanometer-thick hydration shells surrounding charges provide extreme reduction of frictional dissipation as surfaces slide past each other, has emerged as a paradigm for understanding and controlling lubrication in aqueous and biological systems[1-5]. In particular, the highly-hydrated phosphocholine head-groups of phosphatidylcholine (PC) lipids have been shown to act as exceptionally efficient lubrication elements[6-8], readily forming boundary layers with coefficients of friction $\mu < 10^{-2}$ (in the so-called superlubricity regime[9-10]). PC vesicles (liposomes), exposing phosphocholine groups at their outer surface, provide an efficient means of delivering such elements and their associated lubricity to interfaces[11], and have been proposed, via intra-articular injection, for alleviation of lubrication-associated pathologies such as osteoarthritis[12-13]. Liposomes however tend to aggregate with time, and it is essential for their integrity (for example during storage or delivery) that they be stabilized against such aggregation[14-16]. A widely-used approach for this is by steric stabilization, through incorporation of polymer, usually poly(ethylene glycol) (PEG) chains[17-18] (other polymers have also been used[19]), forming a corona about the liposomes that provides an entropic barrier to aggregation. An early study showed that such PEGylation, however, may suppress the very efficient lubrication afforded by the bare (unfunctionalized) phosphocholine-exposing vesicles[20], attributed to the much lower hydration level of the PEG chains. Poly[2-(methacryloyloxy)ethyl phosphorylcholine] (PMPC) as potential alternative to PEG has gained increasing attention not only because of its potential to stabilize colloidal particles[21], but also due to its good lubricity[22].

Here we report the creation of PC vesicles incorporating novel lipid-PMPC conjugates which are fully stable to aggregation and at the same time retain a high-pressure lubricity far superior to that provided by similar but PEGylated vesicles. The idea motivating this design is to use the PMPC chains, which are known to be good lubricants due to their highly-hydrated phosphocholine-like monomers[7, 23], both as steric stabilizers and lubricating molecules simultaneously.

■ MATERIALS AND METHODS

Materials

Distearoylphosphatidylethanolamine-polyethylene glycol (DSPE-PEG, PEG Mw of 5000 Da) were purchased from Avanti polar lipids. Hydrogenated soy phosphatidylcholine (HSPC) and distearoylphosphatidylethanolamine (DSPE) were purchased from Lipoid (Ludwigshafen, Germany). Copper(I) bromide (CuBr, 99.999%), 2-bromoisobutyryl bromide (BIBB, 98%), triethylamine (99%), N,N′,N′,N″,N-pentamethyldiethylenetriamine (PMDETA, 99%), dichloromethane, anhydrous chloroform and silver beads (99.9999%) were purchased from Sigma-Aldrich (Israel). Hydrochloric acid (37%, AR grade) was purchased from Bio-lab (Jerusalem, Israel). 2-(methacryloyloxy)ethyl phosphorylcholine (MPC) was obtained from Vertellus Biomaterials, Basingstoke (U.K.). $NaNO_3$ (ultrapure 99.999%) was purchased from Merk, Germany. Water was highly-purified by a Barnstead Nanopure system and had resistivity 18.2 MΩ and total organic content ca. 1 ppb.

Size Distribution and Zeta Potential

Liposomes were characterized using a Zetasizer Nano-ZS instrument (Malvern Instruments Ltd., Malvern, WR, U.K.) equipped with a red laser at 633 nm set at a scattering angle of 173°. For size distribution and zeta-potential, measurements were carried out at 1 mM liposome concentration dispersed in $NaNO_3$ solution at ca. 150 mM and 10 mM salt concentrations respectively (25 °C, pH 5.8 – 6.2).

Atomic Force Microscopy (AFM)

Liposome covered mica surfaces for imaging were prepared, essentially identically to the preparation of surfaces for the Surface Force Balance studies (see below), as follows. Freshly cleaved mica was placed in a 1 mM SUVs liposome dispersion prepared with 150 mM $NaNO_3$ at room temperature. After overnight incubation, the dispersion surrounding the surfaces was infinitely diluted, by 0.15 M $NaNO_3$ to remove excess liposomes without crossing an air-water interface. Imaging of the surfaces was carried out with an MFP-3D™ Stand Alone (AFM) instrument (Oxford Instruments Asylum Research, Inc., Santa Barbara, CA). No-contact mode scanning in 0.15 M $NaNO_3$ was done using a V-shaped nitride lever having a nominal spring constant of 0.35 N/m with a silicon tips (SNL, Bruker Nano Inc, USA).

Cryo-scanning Electron Microscopy (cryo-SEM)

Liposome covered mica were prepared as described above. Samples were plunged into liquid ethane, and water was sublimed at -80 °C for 2 h. After coating with 3 nm Pt/C, samples were examined by an Ultra 55 SEM (Zeiss, Germany) at a temperature of -120 °C.

Surface Force Balance (SFB) Measurements

The SFB technique and experimental procedure to measure normal (F_n) and shear (F_s) forces between molecularly smooth sheets of mica at separation D have been described in detail previously.[24-25] A schematic is shown in Fig. 1 below.

The mica sheets are half-silvered on their back-side leading to optical interference fringes of equal chromatic order (FECO) when white light is transmitted through them. D is measured (to ±2-3 Å) by monitoring the FECO wavelengths. The normal forces F_n and the lateral forces F_s are evaluated from the bending of the two orthogonal springs of constants K_n and K_s, respectively. Their bending is measured via changes in D (for the normal forces) and changes in the capacitance of an air gap capacitor which yields the bending Δx (for the shear forces, given by $F_s = K_s\Delta x$), respectively. The shear forces are monitored directly through time traces of the air-gap capacitance, as inset to fig. 4b. The mica surfaces were incubated overnight in liposome dispersion (1 mM) in 0.15 M $NaNO_3$, and then rinsed with 0.15 M $NaNO_3$ (see also

(iii) above) and remounted in the SFB. At each surface separation, lateral motion of the top (piezo-mounted) surface was carried out for one minute and the traces monitoring the friction-forces transmitted to the lower surface were recorded (see inset to fig. 4b). The results shown (including fig. S3 below) are based on ten different independent experiments and different contact points within each experiment. Note that for normal force profiles $F_n(D)$, which are the normal forces acting between the two curved mica surfaces a closest separation D apart, the results are normalized as $F_n(D)/R$, where R is the mean radius of curvature of the mica surfaces. In the Derjaguin approximation[1], valid here (R >> D), this yields the interaction energy per unit area between two parallel flat surfaces obeying the same force-distance law.

Synthesis and characterization of DSPE-PMPC

First, DSPE-*2*'-bromoisobutyrate (DSPE-Br) was prepared following the procedure of Li et al.[26] Triethylamine (0.3 mL, 2.35 mmol) was added to 30 mL of dried chloroform containing DSPE (0.88 g, 1.17 mmol), and the mixture was stirred at room temperature for 0.5 h. 2-Bromoisobutyryl bromide (0.115 mL, 1.17 mmol) was then injected into the solution. Then, the mixture was stirred overnight at 40 °C. The solution was washed with water for three times, and the white power was obtained by removing the solvent using rotary evaporator.

DSPE-PMPC was synthesized by atom transfer radical polymerization (ATRP)[27-28] using DSPE-Br as the initiator (Scheme S1). DSPE-Br (87 mg, 0.1 mmol) was dissolved in dichloromethane (3 mL), and MPC (740 mg, 2.5 mmol) monomer was dissolved in ethanol (9 mL). DSPE-Br, MPC and CuBr (14 mg, 0.1 mmol) were added to a Schlenk flask with a magnetic stirrer bar. The flask was degassed by nitrogen for 30 min. Then PMDETA (40 µL, 0.2 mmol) was injected quickly. The flask was stirred for 16 h at 60 °C. Then the solution was dialysis against ethanol and water for 48 h, respectively (CelluSep membrane, MWCO 3500). The polymer DSPE-PMPC was obtained after freeze-drying. ^{1}H NMR (300 MHz, CDCl3/CD_3OD=1/1): chemical shift (ppm): 0.70-1.00 (3H, CH_3−CR−CH_2−), 1.26 (28H, -

$(CH_2)_{14}$-CH_3), 1.75−2.16 (2H, −CH_2−CR−CH_3), 3.34 (9H, −$N^+(CH_3)_3$), 3.75 (2H, −O−CH_2−CH_2−$N^+(CH_3)_3$), 4.07 (2H, −C−O−CH_2−), 4.22 (2H, −CH_2−O−P), 4.31 (2H, −CH_2−CH_2−$N^+(CH_3)_3$).

Preparation of Liposomes

Small unilamellar vesicles (SUVs) were made via a film hydration-extrusion technique[29]. HSPC alone (181 mg), HSPC (178 mg)/DSPE-PMPC (21 mg) or HSPC (178 mg)/DSPE-PEG (20 mg) were dissolved in methanol and chloroform (2 mL, 1:1 v/v). After that, organic solvent was removed by nitrogen overnight. Multilamellar vesicles (MLVs) of modified HSPC were prepared in 0.15 M $NaNO_3$ by sonication for 15 mins at 70 °C, then downsized to form SUVs, ∼70 nm in diameter, at a concentration of 15 mM (by phospholipid concentration), by stepwise extrusion (Northern Lipids Inc., Burnaby, BC, Canada) through polycarbonate membranes starting with 400 nm (5 cycles), 100 nm (6 cycles) and ending with 50 nm (8 cycles).

■ RESULTS AND DISCUSSION

Figure 2b shows the new lipid-PMPC conjugate that we synthesized and its configuration as a stabilizing moiety. We use PC vesicles formed from hydrogenated soy phosphatidylcholine, HSPC, which consists of PC lipids with ca. 85% stearoyl (C_{18}) tails and 15% palmitoyl (C_{16}) tails, and which are known to provide excellent lubrication when in their bare (i.e. non-polymer-incorporating) state[20]. For optimal compatibility, therefore, the molecule for stabilizing such vesicles is made by conjugating the distearoyl part ($(C_{18})_2$) of DSPE, with a PMPC moiety. We functionalize the DSPE with a bromine initiator and then polymerize the MPC via ATRP; the peaks of DSPE-Br initiator (δ = 1.26 ppm) and MPC monomer (δ = 3.75 ppm) determined that the degree of polymerization of DSPE-PMPC is ca. 18 (molecular weight of PMPC ca. 5.3 kDa), as shown in Figure 2a. The resulting molecule is a poly-phosphocholinated lipid analogue. These molecules were then incorporated into SUVs of HSPC, forming liposomes stabilized by PMPC tails (designated HSPC-SUV-PMPC), as indicated in Figure 2b. The PMPCylated SUVs (HSPC-SUV-PMPC) were made via a film hydration-extrusion method at ca. 1.5% mole fraction of the DSPE-PMPC molecules in 0.15 M $NaNO_3$, mimicking physiological level salt concentration (at this low mole fraction any desorption of the DSPE-PMPC molecules is expected to be negligible[30]). HSPC-SUVs that were sterically stabilized with DSPE-PEG conjugates (HSPC-SUV-PEG), also incorporated at 1.5% mole fraction and with the PEG moiety of molecular weight 5000, were similarly made, as were pure HSPC-SUVs with no incorporated polymers, for comparison with the poly-phosphocholinated vesicles.

The stability of the three vesicles types (HSPC-SUV, HSPC-SUV-PMPC and HSPC-SUV-PEG) was determined via dynamic light scattering (DLS) in as shown in Figure 2c. This clearly reveals that the unstabilized HSPC-SUVs are already substantially aggregated within 7 days of preparation, as seen by the shift of the main peak from ca. 70 to ca. 90-100 nm, and the appearance (after 30 days) of a broad secondary peak around 1000 nm diameter. In contrast, both the PEGylated and PMPCylated vesicles remain completely stable (unchanged in size or distribution) for at least 3 months. Zeta (ζ) potential measurements on the stabilized vesicles showed a very small negative potential arising from the charge on the DSPE-PMPC or DSPE-PEG conjugates, but screened almost to neutrality at the physiological-level 0.15 M salt concentration: ζ (HSPC-SUV-PEG) = -2.1±1.2 mV and ζ (HSPC-SUV-PMPC) = -3.2±0.8 mV. Thus, the stability of the PEGylated and PMPCylated vesicles is likely a result of the steric stabilization afforded by the polymer chains rather than due to electrostatic effects.

The behaviour of the PEGylated and PMPCylated liposomes as lubricating boundary layers was examined in a surface force balance (SFB), where normal and shear interactions between two mica surfaces coated with the liposomes are measured directly. The mica substrates were incubated overnight in the respective liposome dispersions, then withdrawn and rinsed in 0.15 M $NaNO_3$ to remove excess dispersion prior to mounting in the SFB. Tapping-mode AFM and cryo-SEM were used to characterize the lipid surface morphology following such incubation and rinsing, as shown in Figure 3. The cryo-SEM images show spherical liposomes above a smooth underlayer. Likewise, the AFM micrographs show some PMPCylated vesicles on top of a smooth bilayer (Figure 3a top), while for the PEGylated vesicles, the scanning by the AFM tip (Figure 3b top) dislodges and removes this top layer of liposomes, revealing the smooth bilayer below. We interpret these micrographs to mean that both PMPCylated and PEGylated vesicles rupture to form bilayers in contact with the mica substrate (height profiles in Figure 3), with loosely-attached intact vesicles on top.

Normal force $F_n(D)$ vs. surface-separation D profiles, and friction force F_s vs. F_n profiles between mica surfaces coated with PEGylated and PMPCylated vesicles are shown in Figure 4. Normalized normal force profiles $F_n(D)/R$ as the surfaces approach are roughly similar for both PEGylated and PMPCylated vesicles. Limiting surface separations D_{lim} at the highest compressions (mean contact pressures up to ca. 100 atm), are 14±3 nm and 12±3 nm for the PEGylated and PMPCylated liposomes respectively (inset to Figure 4a). These indicate a limiting thickness of a little more than one bilayer (of ca. 5 nm thickness) of the lipid on each surface. The repulsion onsets at a separation of ca. 80 nm in the salt solution, similar to its value in salt-free water (broken lines in Figure 4a), pointing to its steric rather than electrostatic origin (as the latter would have been strongly screened in 0.15 M salt). The friction force F_s vs. load F_n variation (Figure 4b) reveals a large difference between the two stabilized liposomes. The PMPCylated-liposome coated surfaces have a friction coefficient which, at $\mu = 0.0006 \sim 0.001$ at the highest pressures, is comparable to non-stabilized HSPC-SUVs[20] (broken line), but is smaller by an order of magnitude or more than that of the surfaces coated by the PEGylated-liposomes (for which $\mu = 0.006 \sim 0.011$). This opens the way to using liposomes as stable, highly efficient lubrication vectors, and is the main new finding of this work.

We understand this as follows. For a mole fraction f of the stabilizing lipid-polymer moiety within the vesicle, the mean distance s between such polymer chains (Figure 2b) is given by $s^2 \approx (a_{\mathrm{lipid}}/f)$, where a_{lipid} is the area occupied by one lipid. The configuration of the polymers and their extension L from the vesicle surface, depends on their surface density and unperturbed coil size R, whether they are brush-like, for $R >> s$, when L > R, or 'mushroom-like' for $R < s$ (in which case L ≈ R). We expect both the PEG and the PMPC moieties to be in good solvent conditions at the room temperature and salt concentration of the experiments[31-32]. We may estimate their size, based on their molecular weight M (≈ 5 kDa), from scattering measurements on free PMPC and PEG chains in similar conditions[31-32]. Dimensions of the PMPC moieties were estimated from the study by Kobayashi et al.[32] For a free PMPC chain of M_n = 234,000, the measured hydrodynamic radius was R_H = 11.5 nm at 0.15 M salt concentration, as in our study, and a small but positive second virial coefficient was measured indicating moderately good solvent conditions. Taking R_H as close to the unperturbed coil size R, and $R \sim M^{3/5}$, yields the estimate $R_{\mathrm{PMPC}} \approx 1.2$ nm (though the asymptotic scaling relation is likely not attained due to the shortness of the PMPC moiety, and this value is probably an underestimate). For the PEG moieties (M = 5 kDa), comparison with Table 2 of ref. [31] for PEG coil dimensions in D_2O/NaCl solution at 25 °C, a coil size of 4.4 nm for M_w = 23.8 kDa scales as above to give the estimate $R_{\mathrm{PEG}} \approx 1.7$ nm. For PC lipids, $a_{\mathrm{lipid}} \approx 0.64$ nm^2 [33], and putting $f = 0.015$ (1.5% mole fraction), we find $s \approx 6.5$ nm. That is, the mean inter-anchor spacing s is considerably larger than the coil size 2R for both the PMPC and the PEG chains emanating from the vesicle, implying a non-overlapping distribution of 'mushroom-like' chain moieties.

Thus the PEGylated and PMPCylated vesicles adsorb to, and rupture on the mica substrate, driven by the dipole-charge attraction between the phosphocholine headgroups and the negatively charged mica substrate. Each such interaction releases a surface-localized counterion into the solution with a corresponding entropy gain, and thus a net attractive energy $\alpha k_B T$ per phosphocholine group interacting with a mica surface charge, where α is of order unity, giving an adhesive energy/unit area of ($-\alpha k_BT/a_{lipid}$). The vesicle adhesion is opposed by the entropic free energy cost of confining the dangling, flexible polymer moieties between the adhered vesicle surface and the mica, modulated by any adsorption energy arising from monomer-mica interactions. The cost of such confinement is βk_BT/(polymer moiety) or ($\beta k_BT/s^2$) in terms of energy/(unit area of the membrane), where β is also of order unity[34]. The overall adhesion energy per unit area of vesicle membrane in contact with the mica substrate is then around [$-(\alpha k_BT/a_{lipid}) + (\beta k_BT/s^2)$]. Since α and β are both of order unity, and since s^2 (~ 40 nm^2) >> a_{lipid} (~ 0.6 nm^2), the net adhesion energy is substantial. This strong adhesion of the vesicle to the surface leads to its rupture, with the resulting coating of each substrate by a lipid bilayer, as indicated in the micrographs (Figure 3 top), with a loosely-attached vesicle layer on top of the bilayer.

As the surfaces approach the loose vesicle layers are removed, and at the highest compressions a lipid bilayer, with its associated flattened polymer moieties, is left on each surface. Its limiting thickness for both PEGylated and PMPCylated vesicles is 6 ~ 7 nm (Figure 4a), slightly higher than the ca. 5 nm expected for a bilayer of HSPC alone; we attribute the 1 ~ 2 nm difference to the compressed polymers on both sides of each bilayer. As the surfaces slide past each other, the hydrated phosphocholine groups exposed by each bilayer slide at the mid-plane with low frictional dissipation due to the hydration lubrication mechanism, as previously observed[6, 20]. The polymer moieties at the mid-plane will also slide past the opposing bilayer and its polymer chains, leading to additional frictional dissipation. For the case of the highly-hydrated PMPC chains such dissipation is known to be very low, as seen in several direct studies[7, 23, 35-36], and is comparable with that between polymer-free lipid bilayers[6, 20]. In contrast, as the flattened PEG moieties slide past each other, they will dissipate frictional energy similar, per chain-chain contact, to that between adsorbed PEG layers, where friction coefficients $\mu_{PEG\text{-}PEG}$ = 0.015±0.005 have been measured[37].

The sliding friction force between two surfaces reflects directly the energy dissipation as they slide past each other. We may consider the friction between two two-component surfaces, such as a lipid bilayer partly covered by a PEG moiety, by summing the different frictional contributions. Consider an area A of the bilayer, of which $a = N_{PEG}.a_{PEG\text{-}monomer}$ is the area covered by PEG monomers, where N_{PEG} is the number of PEG monomers/chain and $a_{PEG\text{-}monomer}$ is the area on the surface occupied by each monomer. A normal load F_n on this area A will be distributed as $F_n[(A - a)/A]$ on the bilayer and $F_n[a/A]$ on the PEG monomers. Each of these components will in turn slide past the opposing surface, which itself consists, on average, of fractions $[(A - a)/A]$ and $[a/A]$ of a bilayer and PEG monomers, feeling frictional forces corresponding to friction coefficients $\mu_{PEG\text{-}PEG}$, $\mu_{bilayer\text{-}bilayer}$ and $\mu_{bilayer\text{-}PEG}$ respectively. Thus on average the total frictional force F_s is given by:

$$F_s = F_n[a/A]\{(a/A)\mu_{PEG\text{-}PEG} + [(A - a)/A].\mu_{PEG\text{-}bilayer}\}$$
$$+ F_n[(A - a)/A]\{(a/A)\mu_{PEG\text{-}bilayer} + [(A - a)/A]\mu_{bilayer\text{-}bilayer}\} \quad (1)$$

where the first term is the frictional force due to the PEG component, and the second due to the bilayer component, of one of the surfaces sliding past the opposing surface. Setting $(a/A) = x$, and rearranging, we find that a simple linear estimate of the friction coefficient $\mu(x)$ expected when a fraction x of each bilayer surface is coated by PEG monomers is given by:

$$F_s/F_n = \mu(x) = x^2\mu_{PEG\text{-}PEG} + (1\text{-}x)^2\mu_{bilayer\text{-}bilayer} + 2x(1\text{-}x)\mu_{bilayer\text{-}PEG} \quad (2)$$

where $\mu_{bilayer\text{-}bilayer} \approx 10^{-3} \sim 10^{-4}$ is the friction coefficient between PC bilayers[6, 20] and $\mu_{bilayer\text{-}PEG}$ is that between a bilayer and an adsorbed-PEG layer. Taking $x = [N_{PEG}a_{PEG\text{-}monomer}/s^2]$, where $N_{PEG} \approx 114$ is the number of PEG monomers/chain and $a_{PEG\text{-}monomer} \approx 0.1$ nm^2 is the area/(PEG monomer)[38]; $\mu_{bilayer\text{-}PEG} = 0.02\pm0.003$[39]; and $\mu_{bilayer\text{-}bilayer} \approx 5\times10^{-4}$ [20] (shown as broken line in Figure 4b), we find $\mu(x) \approx 0.009\pm0.002$ (shaded region in Figure 4b), which is comparable with the friction coefficient values measured for the PEGylated liposomes.

■ CONCLUSIONS

In summary, PMPCylated PC-vesicles represent a class of liposomes forming boundary lubrication layers that are far more efficient than the commonly used PEGylated vesicles, while providing excellent stability against aggregation. This effect arises from the much higher hydration level of the PMPC moieties. Such PMPCylated vesicles have potential as stable, biocompatible lubrication vectors in aqueous media, particularly in high-stress environments (such as joints and artificial joints), for treating lubrication-associated pathologies such as osteoarthritis[13], as well as lubrication of medical implants such as stents and catheters, and in lower-stress environments such as contact lenses to overcome friction-associated discomfort or symptoms of dry-eye syndrome.

■ ACKNOWLEDGMENTS

We thank the European Research Council (AdG CartiLube), the McCutchen Foundation and the Israel Science Foundation- National Science Foundation China joint program (grant ISF-NSFC 2577/17) for their support of this work. We particularly thank Dr. Eyal Shimony for his help with the cryo-SEM images and Dr. Anbumozhi Angayarkanni for sharing data on lipid-bilayer/PEG friction.

■ REFERENCES

1. Raviv, U.; Klein, J., Fluidity of Bound Hydration Layers. *Science* **2002,** *297*, 1540-1543.
2. Donose, B. C.; Vakarelski, I. U.; Higashitani, K., Silica surface lubrication by hydrated cations adsorption from electrolyte solutions. *Langmuir* **2005,** *21*, 1834-1839.
3. Briscoe, W. H.; Titmuss, S.; Tiberg, F.; Thomas, R. K.; McGillivray, D. J.; Klein, J., Boundary lubrication under water. *Nature* **2006,** *444*, 191-194.
4. Ma, L.; Gaisinskaya, A.; Kampf, N.; Klein, J., Origins of hydration lubrication. *Nature Comm.* **2015,** *6*, 6060.
5. Yang, J.; Chen, H.; Xiao, S.; Shen, M.; Chen, F.; Fan, P.; Zhong, M.; Zheng, J., Salt-Responsive Zwitterionic Polymer Brushes with Tunable Friction and Antifouling Properties. *Langmuir* **2015,** *31* (33), 9125-33.
6. Trunfio-Sfarghiu, A.-M.; Berthier, Y.; Meurisse, M.-H.; Rieu, J.-P., Role of Nanomechanical Properties in the Tribological Performance of Phospholipid Biomimetic Surfaces. *Langmuir* **2008,** *24*, 8765–8771.
7. Chen, M.; Briscoe, W. H.; Armes, S. P.; Klein, J., Lubrication at Physiological Pressures by Polyzwitterionic Brushes. *Science* **2009,** *323*, 1698-1702.
8. Raj, A.; Wang, M.; Zander, T.; Wieland, D. C. F.; Liu, X.; An, J.; Garamus, V. M.; Willumeit-Römer, R.; Fielden, M.; Claesson, P. M.; Dėdinaitė, A., Lubrication synergy: Mixture of hyaluronan and

dipalmitoylphosphatidylcholine (DPPC) vesicles. *Journal of Colloid and Interface Science* **2017,** *488*, 225-233.
9. Hod, O.; Meyer, E.; Zheng, Q.; Urbakh, M., Structural superlubricity and ultralow friction across the length scales. *Nature* **2018,** *563* (7732), 485-492.
10. Matta, C.; Joly-Pottuz, L.; De Barros Bouchet, M. I.; Martin, J. M.; Kano, M.; Zhang, Q.; Goddard, W. A., Superlubricity and tribochemistry of polyhydric alcohols. *Physical Review B* **2008,** *78* (8), 085436.
11. Sorkin, R.; Kampf, N.; Dror, Y.; Shimoni, E.; Klein, J., Origins of extreme boundary lubrication by phosphatidylcholine liposomes. *Biomaterials* **2013,** *34*, 5465-5475.
12. Sivan, S.; Schroeder, A.; Verberne, G.; Merkher, Y.; Diminsky, D.; Priev, A.; Maroudas, A.; Halperin, G.; Nitzan, D.; Etsion, I.; Barenholz, Y., Liposomes Act as Effective Biolubricants for Friction Reduction in Human Synovial Joints. *Langmuir* **2010,** *26* (2), 1107-1116.
13. Jahn, S.; Seror, J.; Klein, J., Lubrication of articular cartilage. . *Annu. Rev. Biomed. Eng.* **2016,** *18*, 235-258.
14. Dos Santos, N.; Allen, C.; Doppen, A.-M.; Anantha, M.; Cox, K. A. K.; Gallagher, R. C.; Karlsson, G.; Edwards, K.; Kenner, G.; Samuels, L.; Webb, M. S.; Bally, M. B., Influence of poly(ethylene glycol) grafting density and polymer length on liposomes: Relating plasma circulation lifetimes to protein binding. *Biochimica et Biophysica Acta (BBA) - Biomembranes* **2007,** *1768* (6), 1367-1377.
15. Ishihara, A.; Yamauchi, M.; Kusano, H.; Mimura, Y.; Nakakura, M.; Kamiya, M.; Katagiri, A.; Kawano, M.; Nemoto, H.; Suzawa, T.; Yamasaki, M., Preparation and properties of branched oligoglycerol modifiers for stabilization of liposomes. *Int. J. Pharm.* **2010,** *391* (1), 237-243.
16. Lasic, D. D., Sterically stabilized vesicles. *Angewandte Chemie International Edition in English* **1994,** *33* (17), 1685-1698.
17. Kakkar, A.; Traverso, G.; Farokhzad, O. C.; Weissleder, R.; Langer, R., Evolution of macromolecular complexity in drug delivery systems. *Nature Reviews Chemistry* **2017,** *1* (8), 0063.
18. Torchilin, V. P., Recent advances with liposomes as pharmaceutical carriers. *Nat. Rev. Drug Discov.* **2005,** *4* (2), 145-160.
19. Cao, Z.; Zhang, L.; Jiang, S., Superhydrophilic zwitterionic polymers stabilize liposomes. *Langmuir* **2012,** *28* (31), 11625-32.
20. Goldberg, R.; Schroeder, A.; Silbert, G.; Turjeman, K.; Barenholz, Y.; Klein, J., Boundary Lubricants with Exceptionally Low Friction Coefficients Based on 2D Close-Packed Phosphatidylcholine Liposomes. *Adv. Mat.* **2011,** *23*, 3517-3521.
21. Petroff, M. G.; Garcia, E. A.; Dengler, R. A.; Herrera-Alonso, M.; Bevan, M. A., kT-Scale Interactions and Stability of Colloids with Adsorbed Zwitterionic and Ethylene Oxide Copolymers. *Macromolecules* **2018,** *51* (22), 9156-9164.
22. Chen, M.; Briscoe, W. H.; Armes, S. P.; Klein, J., Lubrication at physiological pressures by polyzwitterionic brushes. *Science* **2009,** *323* (5922), 1698-1701.
23. Iuster, N.; Tairy, O.; Driver, M. J.; Armes, S. P.; Klein, J., Cross-Linking Highly Lubricious Phosphocholinated Polymer Brushes: Effect on Surface Interactions and Frictional Behavior. *Macromolecules* **2017,** *50* (18), 7361-7371.
24. Klein, J.; Kumacheva, E.; Mahalu, D.; Perahia, D.; Fetters, L. J., Reduction of frictional forces between solid surfaces bearing polymer brushes. *Nature* **1994,** *370*, 634.
25. Perkin, S.; Chai, L.; Kampf, N.; Raviv, U.; Briscoe, W.; Dunlop, I.; Titmuss, S.; Seo, M.; Kumacheva, E.; Klein, J., Forces between Mica Surfaces, Prepared in Different Ways, Across Aqueous and Nonaqueous Liquids Confined to Molecularly Thin Films. *Langmuir* **2006,** *22* (14), 6142-6152.
26. Li, Y.; Cheng, Q.; Jiang, Q.; Huang, Y.; Liu, H.; Zhao, Y.; Cao, W.; Ma, G.; Dai, F.; Liang, X.; Liang, Z.; Zhang, X., Enhanced endosomal/lysosomal escape by distearoyl phosphoethanolamine-polycarboxybetaine lipid for systemic delivery of siRNA. *J. Control. Release* **2014,** *176*, 104-114.
27. Matyjaszewski, K.; Xia, J., Atom transfer radical polymerization. *Chem. Rev.* **2001,** *101* (9), 2921-2990.
28. Du, J.; Tang, Y.; Lewis, A. L.; Armes, S. P., pH-sensitive vesicles based on a biocompatible zwitterionic diblock copolymer. *J. Am. Chem. Soc.* **2005,** *127* (51), 17982-17983.
29. Cao, Z.; Zhang, L.; Jiang, S., Superhydrophilic zwitterionic polymers stabilize liposomes. *Langmuir* **2012,** *28* (31), 11625-11632.
30. Mineart, K. P.; Kelley, E. G.; Nagao, M.; Prabhu, V. M., Processing–structure relationships of poly (ethylene glycol)-modified liposomes. *Soft Matter* **2017,** *13* (31), 5228-5232.
31. Alessi, M. L.; Norman, A. I.; Knowlton, S. E.; Ho, D. L.; Greer, S. C., Helical and Coil Conformations of Poly(ethylene glycol) in Isobutyric Acid and Water. *Macromolecules* **2005,** *38* (22), 9333-9340.

32. Kobayashi, M.; Terayama, Y.; Kikuchi, M.; Takahara, A., Chain dimensions and surface characterization of superhydrophilic polymer brushes with zwitterion side groups. *Soft Matter* **2013,** *9* (21), 5138-5148.
33. van Meer, G.; Voelker, D. R.; Feigenson, G. W., Membrane lipids: where they are and how they behave. *Nat. Rev. Mol. Cell. Biol.* **2008,** *9*, 112.
34. de Gennes, P. G., *Scaling Concepts in Polymer Physics*. Cornell Univ. Press, Ithaca: N.Y., 1979.
35. Banquy, X.; Burdyńska, J.; Lee, D. W.; Matyjaszewski, K.; Israelachvili, J., Bioinspired Bottle-Brush Polymer Exhibits Low Friction and Amontons-like Behavior. *J. Am. Chem. Soc.* **2014,** *136* (17), 6199-6202.
36. Tairy, O.; Kampf, N.; Driver, M. J.; Armes, S. P.; Klein, J., Dense, Highly Hydrated Polymer Brushes via Modified Atom-Transfer-Radical-Polymerization: Structure, Surface Interactions, and Frictional Dissipation. *Macromolecules* **2015,** *48*, 140-151.
37. Chai, L.; Klein, J., Shear Behavior of Adsorbed Poly(ethylene Oxide) Layers in Aqueous Media. *Macromolecules* **2008,** *41*, 1831-1838.
38. *Polymer Handbook*, J. Brandrupp and E.H. Immergut, eds.; Wiley, New York 4th Edition (1999).
39. A. Angayarkanni and J. Klein, Private Communication.

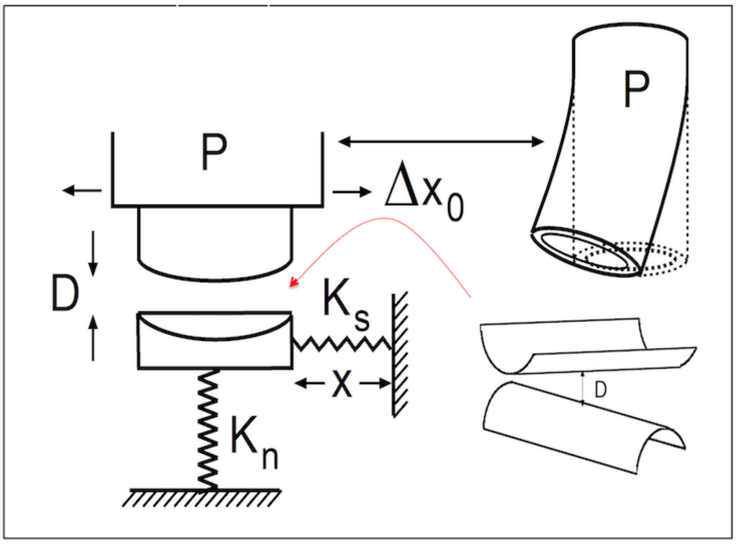

Figure 1. Schematic of the SFB[24-25], where the top surface mounted on a sectored piezo-tube P can move normally and laterally, and normal and shear forces are directly measured through bending of respective orthogonal springs K_n and K_s.

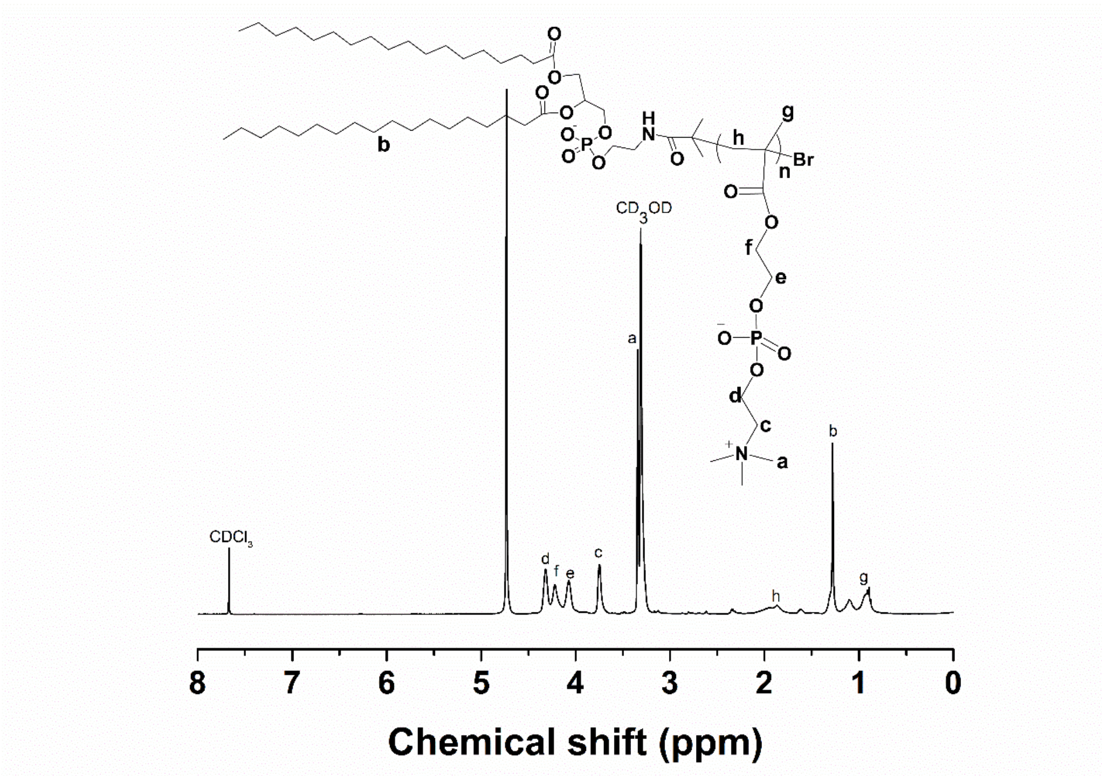

(a)

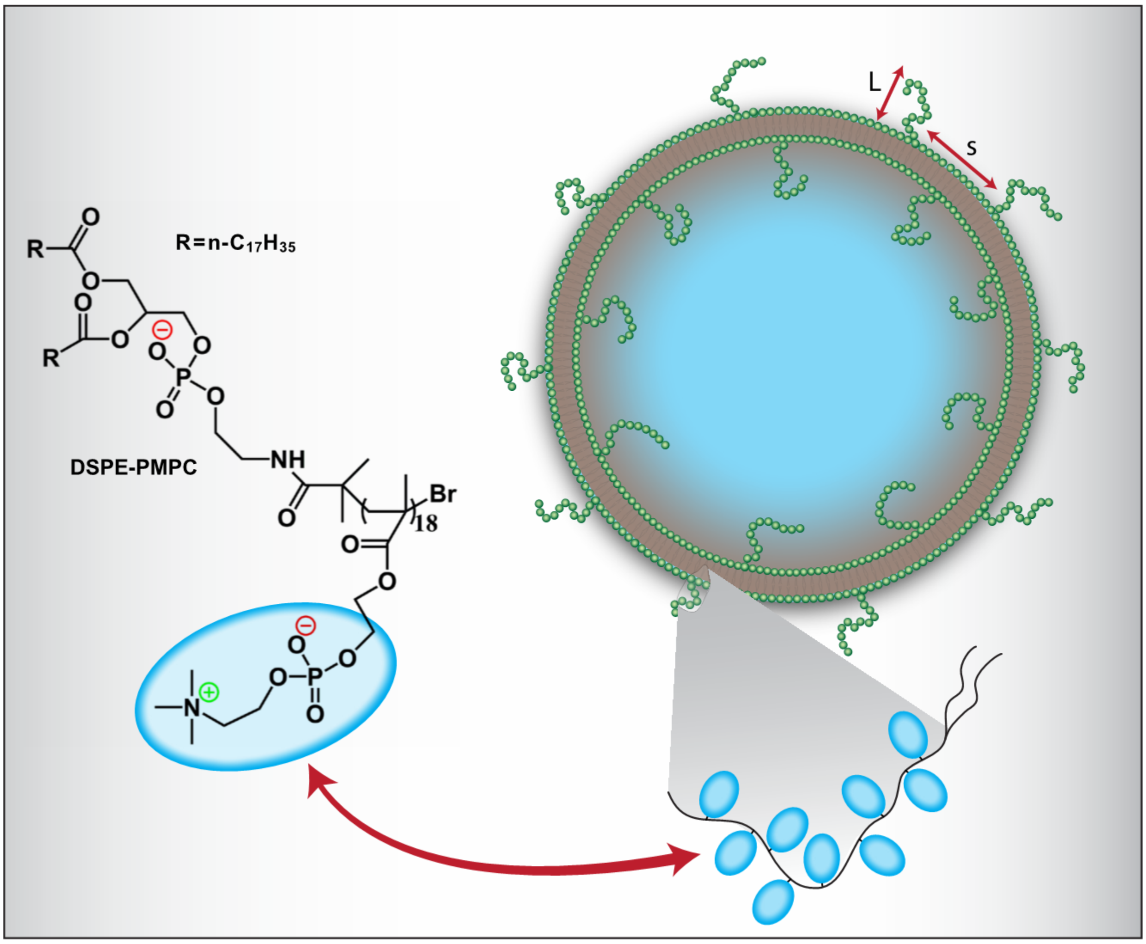

(b)

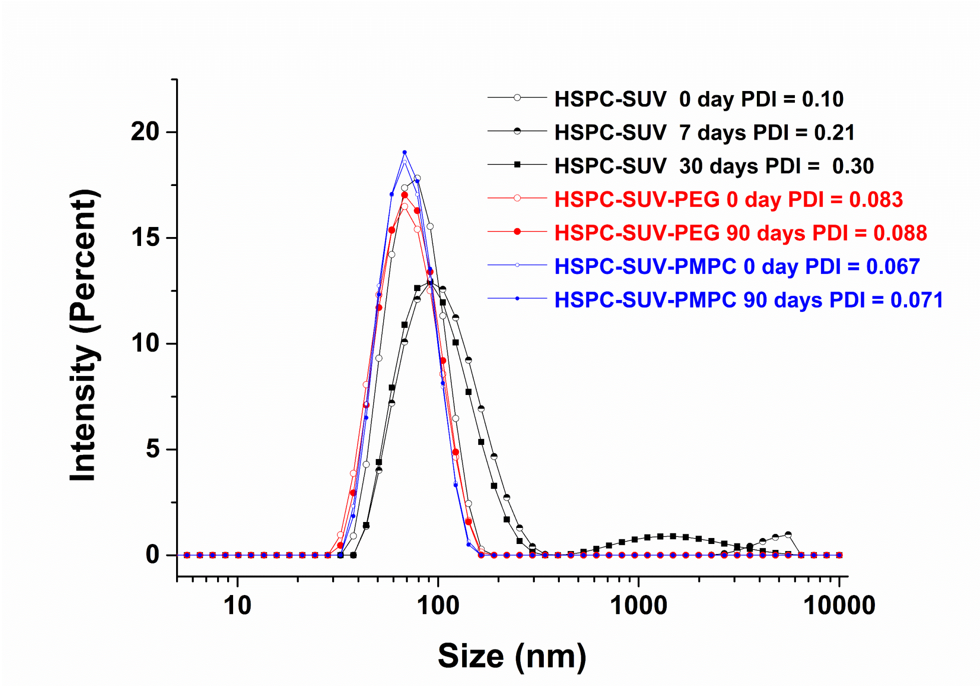

(c)

Figure 2. (a) [1]H-NMR characterization of DSPE-PMPC. (b) Showing the lipid-PMPC conjugate and its incorporation in a PC vesicle. (c) DLS-determined size distribution, of HSPC-SUVs, either bare or

stabilized by PMPC or by PEG moieties, in 0.15 M $NaNO_3$, at different times following preparation. Measurements were at 1 mM liposome concentration.

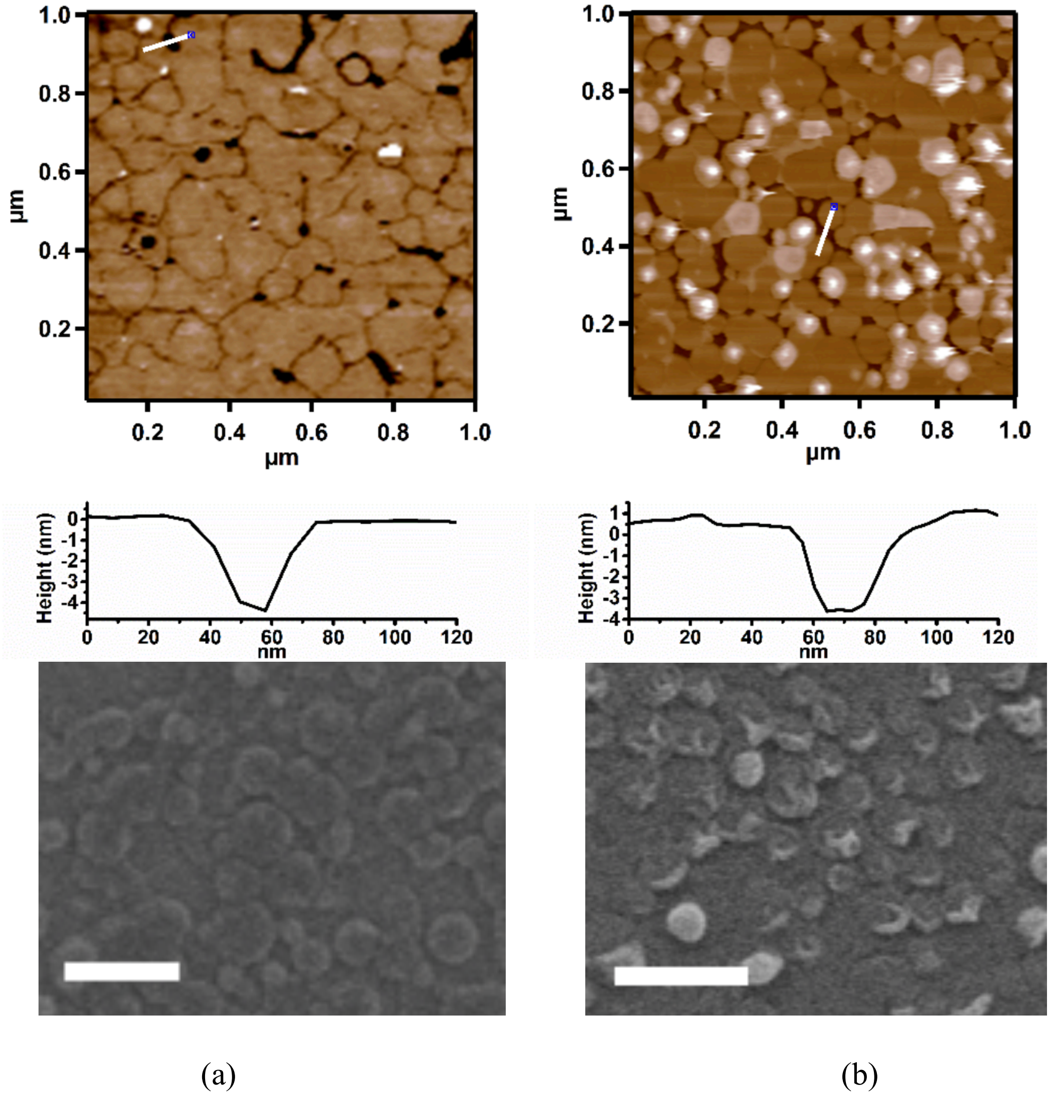

Figure 3. Tapping-mode AFM (top) and cryo-SEM (bottom) images of mica following adsorption and washing of a) HSPC-SUV-PEG and b) HSPC-SUV-PMPC vesicles. Scale bars: 200 nm. Similar images were obtained at several different points on the respective mica surfaces.

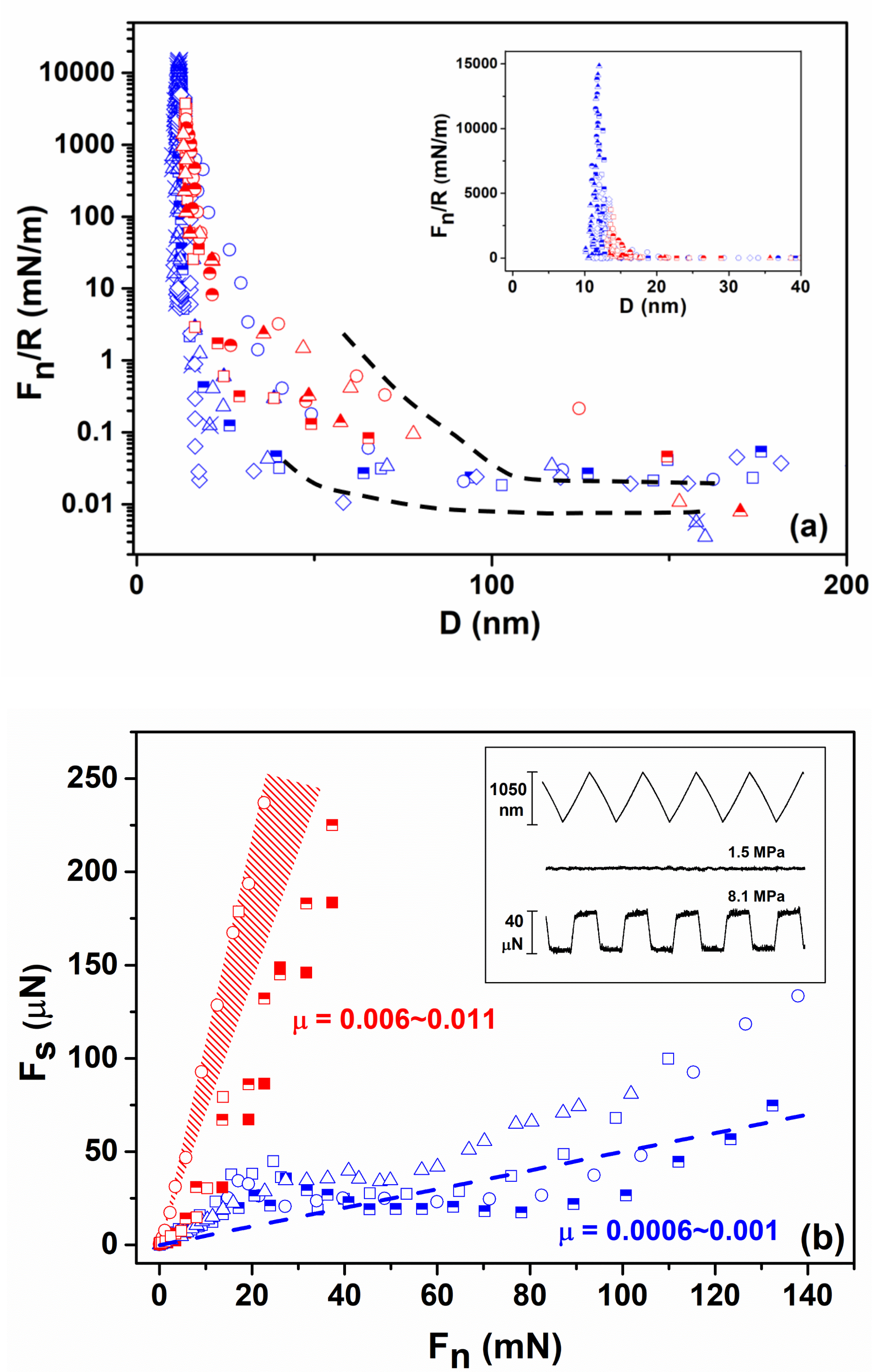

Figure 4. (a) Normalized force profiles $F_n(D)/R$ between HSPC-SUV-PEG (red) and HSPC-SUV-PMPC layers (blue) in 150 mM $NaNO_3$. R is the mean radius of curvature of the mica sheets. Inset shows 'hard wall' separations on expanded scale. Broken lines are $F_n(D)/R$ range in pure water (SI). (b) frictional forces F_s vs. F_n between HSPC-SUV-PEG (red) and HSPC-SUV-PMPC layers (blue), where the range of given for each system is based on the extremal data points. The inset shows F_s, lower 2 traces, as a function of applied sliding motion, top trace. Shaded region (μ = 0.009±0.002) is from eq (2). Broken line: characteristic HSPC bilayer-bilayer friction based on experimentally-measured values

from ref.[20]. Different shaped symbols correspond to different contact positions with first approaches (empty symbols) and second approaches (filled symbols).

Table of Contents

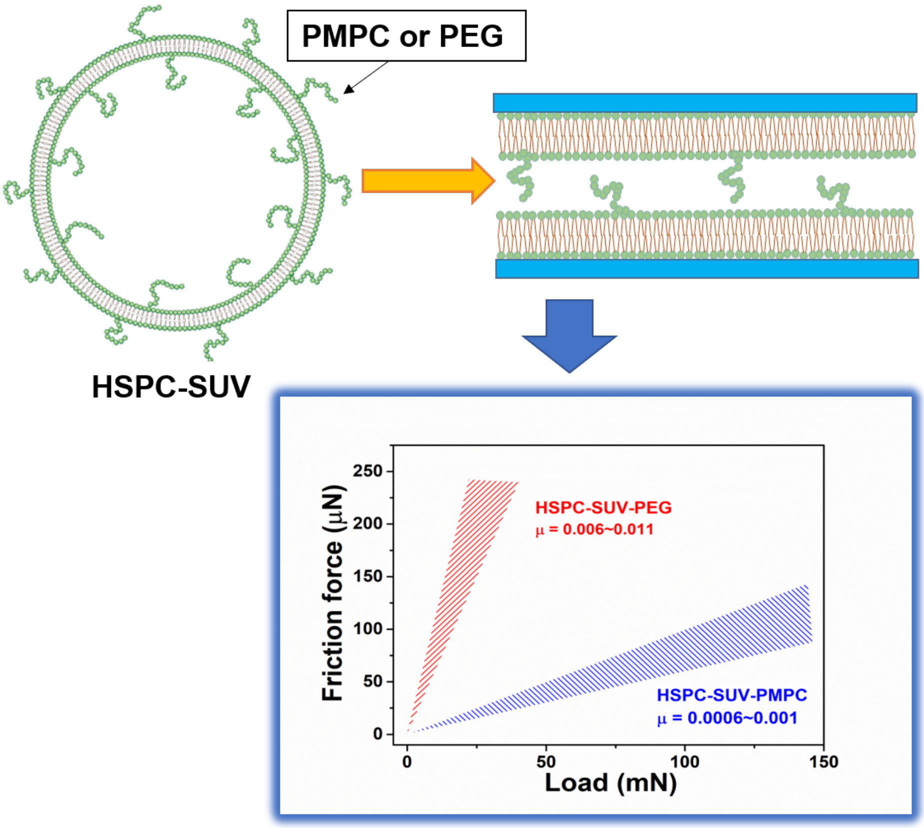

Stable Superlubrication Vector: A new class of stabilized liposomes, incorporating a novel lipid/poly(2-methacryloyl phosphorylcholine) (PMPC) conjugate, are stable to aggregation and at the same time act as superlubric vectors, reducing friction in physiological conditions by an order of magnitude or more relative to PEGylated vesicles (the most commonly used stabilizers), due to the much higher hydration of the PMPC moieties.

Supplementary Information

Poly-phosphocholinated Liposomes Form Stable Superlubrication Vectors

Weifeng Lin[1], Nir Kampf[1], Ronit Goldberg[1], Michael J. Driver[2], Jacob Klein[1]*

[1]Department of Materials and Interfaces, Weizmann Institute of Science, Rehovot 76100, Israel.

[2] Vertellus Biomaterials, Vertellus Specialties UK Ltd., Basingstoke, Hampshire RG25 2PH, U.K.

*** Corresponding author:**

E-mail address: jacob.klein@weizmann.ac.il

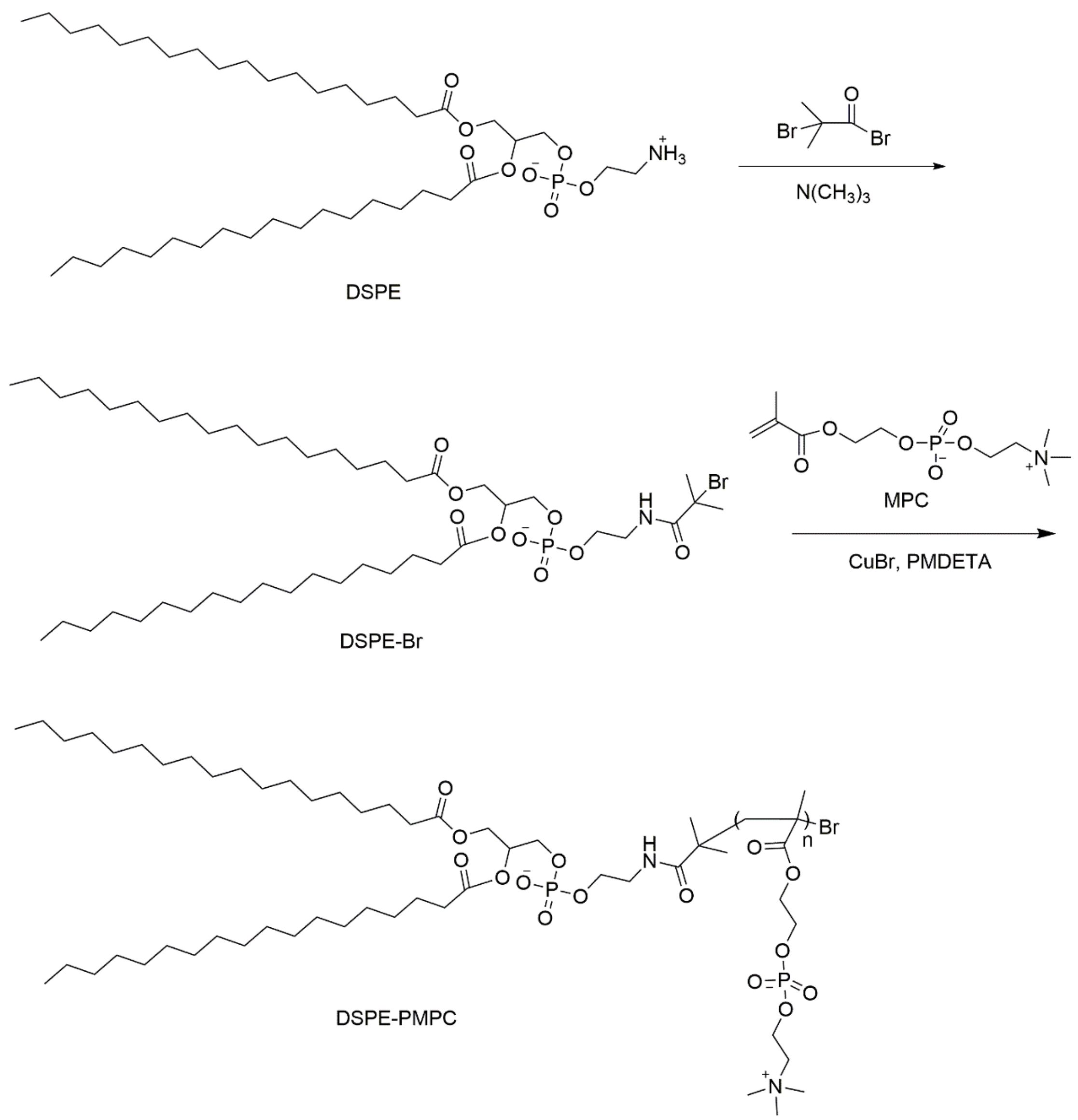

Scheme S1. Schematic illustration of the preparation of DSPE-PMPC polymer via atom transfer radical polymerization, as described in main text.

Control measurements in pure water

As controls, force profiles were measured between mica surfaces coated with PEGylated and PMPCylated vesicles, prepared in high-purity water with no added salt. These are shown in fig. S1. The curves are a guide to the eye delineating the bulk of the data, and, for the region of onset of interactions ($D \approx 150 - 50$ nm), are reproduced as broken curves in fig. 4a in the main text. Comparison shows that the onset distance for the repulsion was similar both in 0.15 M salt and in no-added-salt water, revealing the steric rather than electrostatic nature of the interaction, since the latter would be strongly reduced at the high salt concentration.

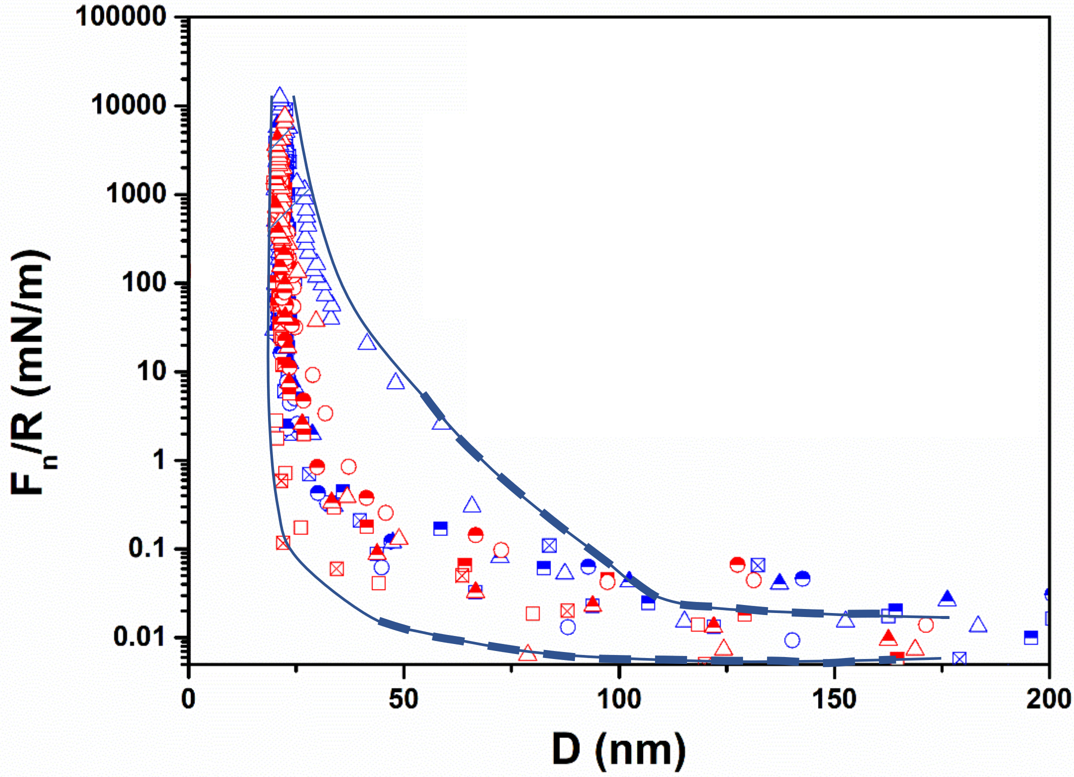

Figure S1. Force distance profiles between mica surfaces coated with PEGylated (blue) and PMPCylated (red) HSPC vesicles, in high purity water with no added salt. The solid curves are a guide to the eye. The onset region from ca. 50 to ca. 150 nm, overlaid by bold broken lines, is reproduced in fig. 4a of the main text. Different shaped symbols correspond to different contact positions with first approaches (empty symbols), second approaches (filled symbols), and retraction profile (crossed symbols).